Single-ion scaling of the low-temperature properties of f-electron materials with non-Fermi-liquid groundstates

1996 J. Phys.: Condens. Matter 8 9773

(http://iopscience.iop.org/0953-8984/8/48/008)

J. Phys.: Condens. Matter **8** (1996) 9773–9791. Printed in the UK

Single-ion scaling of the low-temperature properties of f-electron materials with non-Fermi-liquid groundstates

M B Maple†‡§‖, R P Dickey†‡, J Herrmann‡, M C de Andrade‡, E J Freeman†‡, D A Gajewski†‡and R Chau†‡

† Department of Physics, University of California at San Diego, La Jolla, CA 92093-0319, USA
‡ Institute for Pure and Applied Physical Sciences, University of California at San Diego, La Jolla, CA 92093-0360, USA
§ Institute for Theoretical Physics, University of California at Santa Barbara, Santa Barbara, CA 93106-4030, USA

Received 20 September 1996

Abstract. Certain chemically substituted Ce and U compounds have low-temperature physical properties that exhibit non-Fermi-liquid (NFL) characteristics and apparently constitute a new class of strongly correlated f-electron materials. The NFL behaviour takes the form of weak power law or logarithmic divergences in the temperature dependence of the physical properties that scale with a characteristic temperature T_0, which, in some systems, can be identified with the Kondo temperature T_K. These systems have complex temperature T–chemical substituent composition x phase diagrams, which contain regions displaying the Kondo effect, NFL behaviour, spin glass freezing, magnetic order, quadrupolar order, and, sometimes, even superconductivity. Possible origins of the NFL behaviour include a multichannel Kondo effect and fluctuations of an order parameter in the vicinity of a second-order phase transition at $T = 0$ K. Recent experiments on the systems $Y_{1-x}U_xPd_3$ and $U_{1-x}M_xPd_2Al_3$ (M = Th, Y) are reviewed. In the $Y_{1-x}U_xPd_3$ and $U_{1-x}Th_xPd_2Al_3$ systems, the low-temperature physical properties in the NFL regime scale with the U concentration and T_K, suggesting that single-ion effects are responsible for the NFL behaviour.

1. Introduction

A new class of strongly correlated f-electron materials whose low-temperature physical properties display non-Fermi-liquid (NFL) behaviour has attracted a great deal of attention during recent years [1–4]. The f-electron materials of interest are Ce and U intermetallic compounds which, with a few possible exceptions, have been alloyed with a nonmagnetic element. (However, there is evidence for NFL behaviour in a few unsubstituted f-electron compounds such as UBe_{13} [5, 6] and Ce_7Ni_3 [7].) The Ce and U ions carry magnetic dipole or electric quadrupole moments that interact with the spins and charges of the conduction electrons, giving rise to a Kondo effect, magnetic and/or quadrupolar ordering, and NFL behaviour at low temperature. The nonmagnetic elements, which can be substituted on either f-element or non-f-element sublattices, serve to access the NFL regime, presumably through changes in average electron concentration, the introduction of chemical disorder, etc. In these materials, the NFL behaviour takes the form of weak power law or logarithmic divergences in the temperature dependence of the physical properties at low temperatures

‖ Corresponding author: M B Maple, Physics Department 0319, University of California at San Diego, 9500 Gilman Drive, La Jolla, CA 92093-0319, USA; e-mail address: mbmaple@ucsd.edu

0953-8984/96/489773+19$19.50

$T \ll T_0$, where T_0 is a characteristic scaling temperature. This suggests the existence of a quantum critical point at $T = 0$ K, possible origins of which include an unconventional moment screening process, such as a multichannel Kondo effect [8], and fluctuations of an order parameter in the vicinity of a second-order phase transition at $T = 0$ K [9].

The electrical resistivity ρ, specific heat C, and magnetic susceptibility χ of many of the f-electron systems have the following NFL temperature dependences for $T \ll T_0$ [1, 2]: $\rho \sim 1 - a(T/T_0)$, where $|a| \approx 1$ and $a < 0$ or > 0, $C(T)/T \sim (-1/T_0)\ln(T/T_0)$, and $\chi(T) \sim 1 - (T/T_0)^{1/2}$ or $\chi(T) \sim -\ln(T/T_0)$. In several of the f-electron systems, including the $Y_{1-x}U_xPd_3$ and $U_{1-x}Th_xPd_2Al_3$ systems considered herein, the characteristic temperature T_0 can be identified with the Kondo temperature T_K. The new NFL f-electron materials can be contrasted with 'conventional' heavy-fermion f-electron compounds, such as $CeAl_3$ and UPt_3, which behave as Fermi liquids [10], in spite of the strong electron–electron interactions that renormalize the effective mass of the electron by a factor of $\sim 10^2$–10^3! (Equivalently, the effective Fermi temperature T_F is low, $\sim$ 1–10 K!) Here, the temperature and frequency dependences of the physical properties scale with T_F. The quantities ρ, C, and χ have the following familiar forms for $T \ll T_F$: $\rho(T) \sim 1 - a(T/T_F)^2$, where $|a| \approx 1$ and $a > 0$ or < 0, $C(T)/T \sim \gamma_0$ (where γ_0 can be as large as $\sim 1\,\mathrm{J\,mol^{-1}K^2}$!), and $\chi(T) \sim \chi_0$ such that $\chi_0/\gamma_0 \sim 1$.

As we have previously noted [2], interest in NFL behaviour in strongly correlated electron systems has been partially driven by interest in the unconventional superconductivity found in two classes of materials, the layered cuprates and the heavy-fermion f-electron materials [10]. In spite of the enormous disparity in the values of the superconducting transition temperature T_c, which are as high as $\sim$ 133 K for the cuprate superconductors but $\lesssim$2 K for the heavy-fermion f-electron materials, the superconducting states of these materials share some striking similarities—the superconducting state appears to be anisotropic, with an energy gap that may vanish at points or along lines on the Fermi surface, and the superconducting electron pairing may be mediated by antiferromagnetic spin fluctuations. An understanding of the source of the NFL behaviour in these systems could provide important information about the electronic structure and excitations of these systems, as well as the origin of the unconventional superconductivity.

In this paper, we briefly review the current experimental situation for the archetypal system $Y_{1-x}U_xPd_3$ and the systems $U_{1-x}M_xPd_2Al_3$ (M = Th,Y). These systems exhibit complex T–x phase diagrams in which various phenomena such as spin glass, magnetic and/or quadrupolar order, superconductivity, the Kondo effect, and NFL behaviour are found. In the NFL regime, in which we are primarily interested, the NFL characteristics scale with x and T_K, suggesting that the origin of the NFL behaviour is a single-ion mechanism that is related to an unconventional Kondo effect.

2. The $Y_{1-x}U_xPd_3$ system

The archetypal f-electron system whose physical properties display NFL characteristics at low temperatures is $Y_{1-x}U_xPd_3$, the first f-electron system in which NFL behaviour was observed [8] and the one that has been studied the most extensively. In the original investigations on this system, that were carried out at UCSD [11], the electrical resistivity ρ, specific heat C, and magnetization M were measured as functions of temperature T and magnetic field H on polycrystalline $Y_{1-x}U_xPd_3$ specimens with U concentrations x spanning the entire range $0 \leqslant x \leqslant 1$. The low-temperature behaviour of $\rho(T)$, $C(T)$, and $\chi(T)$ in the range $0 \leqslant x \leqslant 0.55$, where the system crystallizes in the cubic Cu_3Au crystal structure, was found to be generally consistent with the predictions of the quadrupolar

Kondo model, given the level of understanding of the model at that time [12]. On the other hand, Andraka and Tsvelik [13] performed similar measurements of ρ, C, and M as functions of T and H on a specimen of composition $x = 0.2$ and arrived at a quite different interpretation. From the scaling behaviour of $C(T, H)$ and $\chi(T, H)$ with H/T, they concluded that the NFL behaviour was due to fluctuations of an order parameter in the vicinity of a second-order phase transition at $T = 0$ K. In the meantime, extensive investigations on the $Y_{1-x}U_xPd_3$ system have been carried out and have revealed that the experimental situation is considerably more complex, as we briefly describe in the following.

3. The low-temperature phase diagram of the $Y_{1-x}U_xPd_3$ system

Shown in figure 1 is the most recent version of the low-temperature T–x phase diagram of the $Y_{1-x}U_xPd_3$ system that was first reported in [1]. The $Y_{1-x}U_xPd_3$ system is derived from the parent compound UPd_3 by substituting Y for U. UPd_3, which crystallizes in the hexagonal Ni_3Ti structure, is itself quite interesting since it is one of the few metallic actinide compounds whose properties are all consistent with localized f electrons. Sharp crystalline electric field (CEF) levels are observed that are indicative of an f^2 nonmagnetic ground state and of tetravalent U ions [14]. The linear coefficient of the low-temperature specific heat $\gamma \sim 1\,\text{mJ mol}^{-1}\text{K}^{-2}$ is typical of a normal metal [15]. Photoemission spectroscopy (PES) and bremsstrahlung isochromat spectroscopy (BIS) measurements reveal a gap around the Fermi level E_F with 5f peaks below and above E_F [16]. According to a recent inelastic neutron scattering study, UPd_3 undergoes a quadrupolar transition at 6.5 K, followed by a magnetic transition at 4.5 K [17].

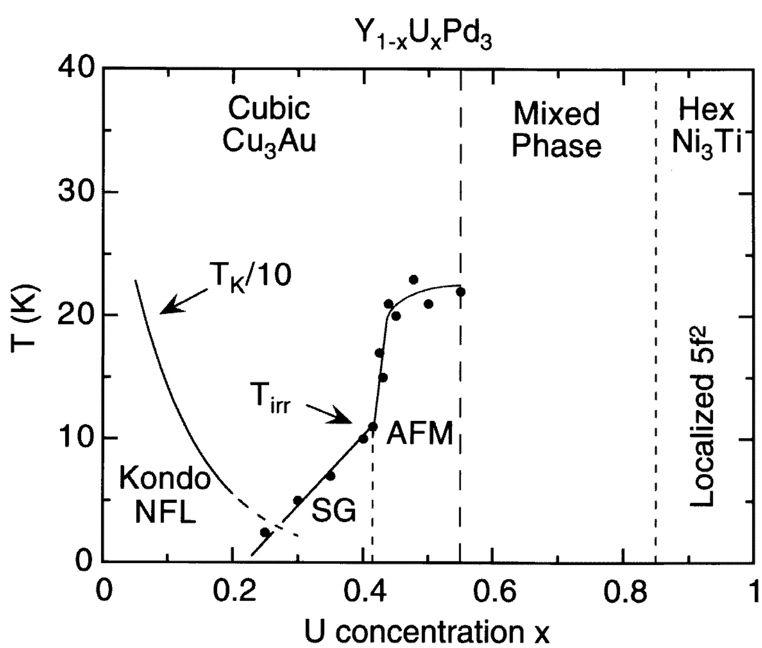

Figure 1. Low-temperature T–x phase diagram for the $Y_{1-x}U_xPd_3$ system.

Of particular interest are the physical properties of $Y_{1-x}U_xPd_3$ in the cubic Cu_3Au phase that extends from $x = 0$ to $x \approx 0.55$. Magnetization $M(T)$ measurements on $Y_{1-x}U_xPd_3$ samples, performed under field-cooling and zero-field-cooling conditions, exhibit irreversible behaviour reminiscent of spin glass (SG) freezing below an irreversibility temperature T_{irr} in the U concentration range $0.2 \lesssim x \lesssim 0.55$. A plot of T_{irr} against x in figure 1 delineates two regions, one in the range $0.2 \leqslant x \leqslant 0.43$ and the other in the range $0.43 \leqslant x \leqslant 0.55$, where the U magnetic moments undergo spin glass freezing and antiferromagnetic (AFM) ordering, respectively. Long-range AFM ordering of the U moments was first observed by neutron scattering experiments on a sample with $x = 0.45$ [18]. Spin glass freezing and antiferromagnetic ordering in the $Y_{1-x}U_xPd_3$ system have been established by means of a variety of measurements including μSR [19], magnetic relaxation [20, 21], ac magnetic susceptibility [20], nonlinear magnetic susceptibility [21], electrical resistivity [20], and specific heat [20].

Our primary interest is in the part of the T–x phase diagram in the range $0 < x \lesssim 0.2$ where the physical properties of $Y_{1-x}U_xPd_3$ display an unconventional Kondo effect with NFL behaviour at low temperatures [11, 22]. As indicated in figure 1, the Kondo temperature T_K decreases rapidly with increasing x, which has been attributed to 'Fermi level tuning', as described below.

4. The Kondo effect and Fermi level tuning of the Kondo temperature

Electrical resistivity $\rho(T)$ measurements on the $Y_{1-x}U_xPd_3$ system in the Cu_3Au phase ($0 \leqslant x \leqslant 0.55$) reveal the occurrence of a Kondo effect. Shown in figure 2(*a*) are ρ–T data for $Y_{1-x}U_xPd_3$ specimens with various values of x ranging from 0 to 0.5; the increase of ρ with decreasing T indicates the occurrence of the Kondo effect. Plots of $\Delta\rho(T)/\Delta\rho(0)$ against $\log T$ for $Y_{1-x}U_xPd_3$ samples with $x = 0.02$, 0.05, 0.1, and 0.2 are shown in figure 2(*b*). Here, $\Delta\rho(T)$ is the contribution to $\rho(T)$ associated with the scattering of electrons by the U ions, obtained by subtracting from $\rho(T)$ a phonon contribution estimated from $\rho(T)$ of YPd_3. We identify the Kondo temperature T_K with the temperature at which $\Delta\rho(T)$ starts to deviate from a $\log T$ dependence which is consistent with the criterion $\Delta\rho(T_K)/\Delta\rho(0) \equiv 0.8$ which we use to define T_K. The values of T_K obtained from this criterion are plotted against x in the inset of figure 2(*b*).

Magnetic susceptibility measurements on the $Y_{1-x}U_xPd_3$ system are also consistent with the occurrence of a Kondo effect. Displayed in figure 3(a) are plots of $(\chi - \chi_0)^{-1}$ against T for $Y_{1-x}U_xPd_3$ between $\sim$2 K and 300 K, where χ_0 was determined by fitting the $\chi(T)$ data to the sum of a constant χ_0 and a Curie–Weiss law. Below $\sim$100 K, the $(\chi - \chi_0)^{-1}$ against T data fall below the linear fits to the higher-T data and approach a finite value as $T \to 0$, indicative of a nonmagnetic ground state. The values of the effective moment μ_{eff} and the Curie–Weiss temperature θ_p extracted from the Curie–Weiss fits in figure 3(a) are plotted against x in figure 3(b). The effective moment $\mu_{eff} \approx 3.1\,\mu_B$ is smaller than the free ion value of $3.58\,\mu_B$/U ion for tetravalent U, and the Curie–Weiss temperature θ_p is negative. A reduced value of μ_{eff} and a negative θ_p are both characteristic of systems which exhibit a Kondo effect where $-\theta_p = cT_K$ with $c \approx 3$–4. The decrease of $|\theta_p|$ with x is consistent with the decrease of T_K inferred from the $\Delta\rho(T)/\Delta\rho(0)$ data shown in figure 2(b).

The decrease of the Kondo temperature T_K with increasing x, indicated in figure 1, has been attributed to 'Fermi level tuning', a phenomenon in which the U^{4+} 5f binding energy $\varepsilon_{5f} = E_F - E_{5f}$, where E_F is the Fermi energy and E_{5f} is the energy of the U^{4+} 5f state, increases continuously by $\sim$1 eV as x increases from zero to one [1, 22]. The increase of ε_{5f} with x was discovered in photoemission studies of $Y_{1-x}U_xPd_3$ [23] and can be understood in terms of the increase of E_F with x as tetravalent U is substituted for

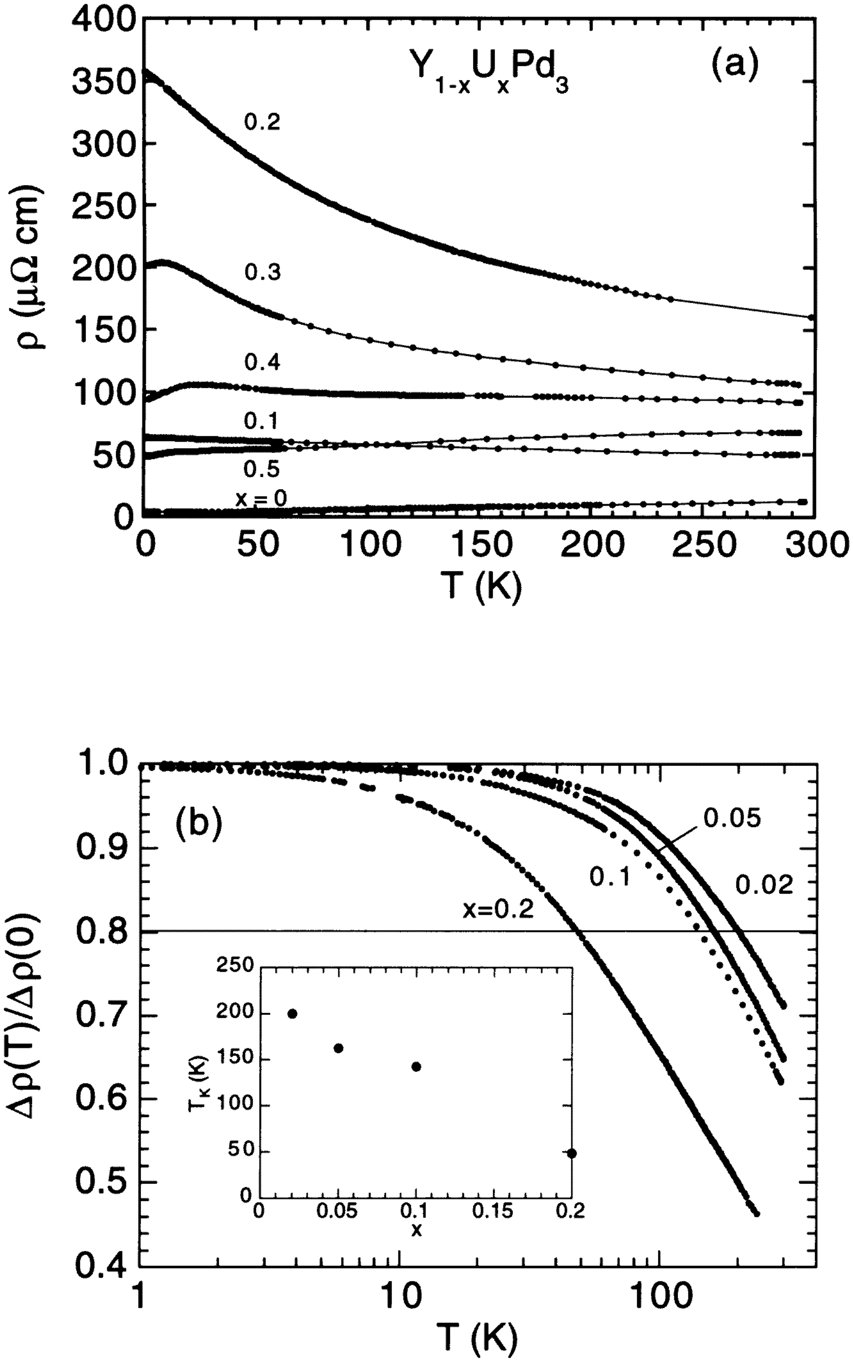

Figure 2. (a) Electrical resistivity ρ against temperature T of $Y_{1-x}U_xPd_3$ for various values of x in the range $0 \leqslant x \leqslant 0.5$. (b) U contribution to the electrical resistivity, $\Delta\rho$, of $Y_{1-x}U_xPd_3$ ($x = 0.02$, 0.05, 0.1, 0.2), normalized to the extrapolated zero-temperature value $\Delta\rho(0)$, against $\log T$. Inset: Kondo temperature T_K, where T_K is defined as $\Delta\rho(T_K)/\Delta\rho(0) \equiv 0.8$ (indicated by the horizontal line in the figure).

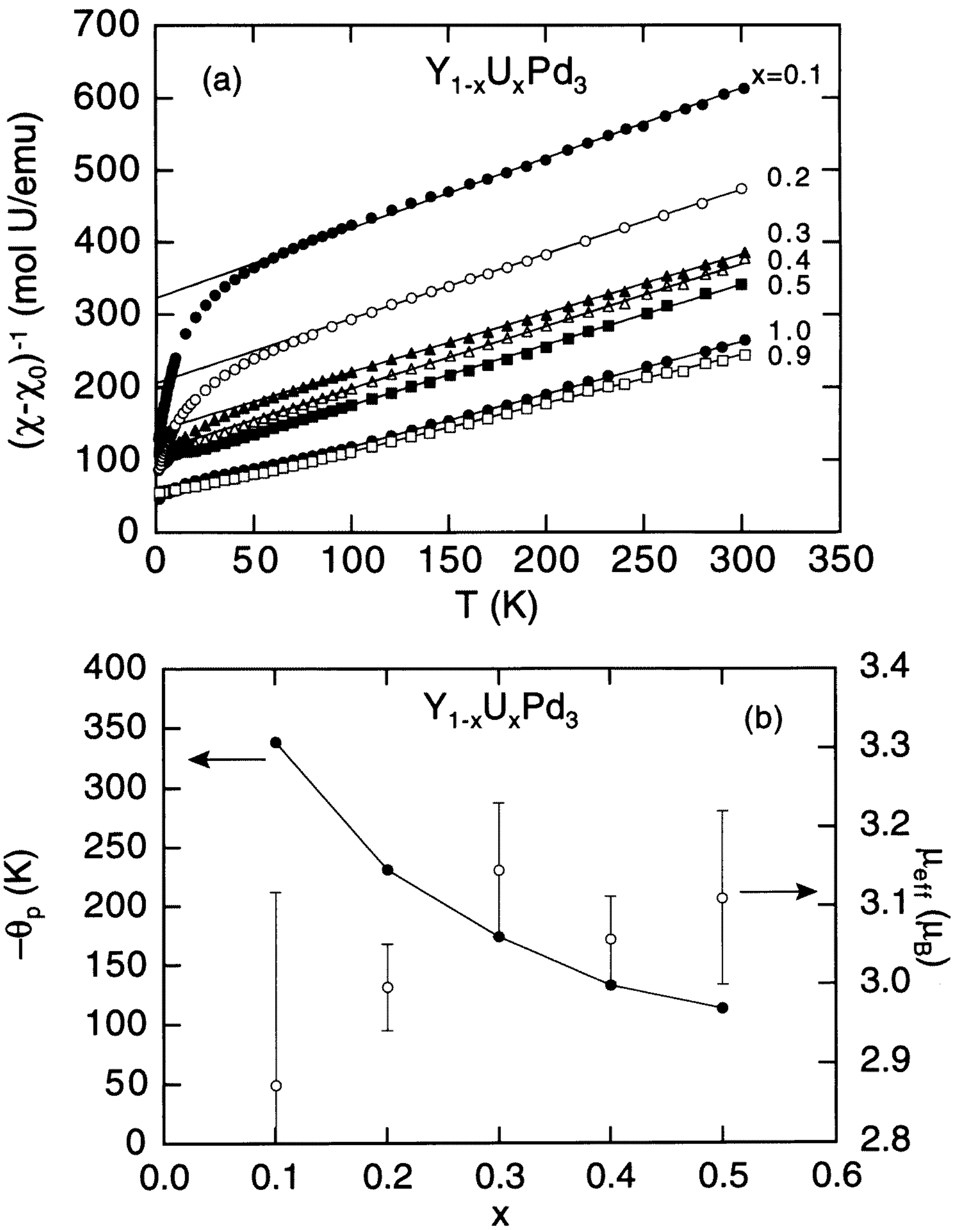

Figure 3. (a) Inverse of the U contribution to the magnetic susceptibility $(\chi - \chi_0)^{-1}$ against T for $Y_{1-x}U_xPd_3$ for various values of x in the range $0 \leqslant x \leqslant 1$. The lines are fits to a Curie–Weiss law for 100 K $\leqslant T \leqslant$ 300 K. (b) Magnitude of the Curie–Weiss temperature $-\theta_p$ and effective magnetic moment μ_{eff} against x for $Y_{1-x}U_xPd_3$, determined from the Curie–Weiss fits in (a).

trivalent Y. The nearly linear increase of ε_{5f} with x should cause a rapid decrease in T_K since

$$T_K \sim T_F \exp[-1/N(E_F)|\mathcal{J}|] \sim T_F \exp[-\varepsilon_{5f}/\langle V_{kf}^2\rangle N(E_F)] \qquad (1)$$

where T_F is the Fermi temperature, $N(E_F)$ is the density of states at E_F, $\mathcal{J} \sim -\langle V_{kf}^2\rangle/\varepsilon_{5f}$ is the exchange interaction parameter, and V_{kf} is the hybridization matrix element. Assuming that ε_{5f} increases linearly with x (i.e. $\varepsilon_{5f} \sim \varepsilon_0+\varepsilon_1 x$) and that $\langle V_{kf}^2\rangle$ remains approximately constant, it follows that

$$T_K \sim (T_K)_0 \exp(-\alpha x) \tag{2}$$

where $(T_K)_0$ is the value of T_K for $x \to 0$ and $\alpha = \varepsilon_1/\langle V_{kf}^2\rangle N(E_F)$ [24].

5. Single-ion scaling of the low-temperature physical properties

Striking NFL characteristics are found in $\rho(T)$, $C(T)$, and $\chi(T)$ of $Y_{1-x}U_xPd_3$ at low temperatures $T \ll T_K$, which scale with T_K. Here, T_K has been inferred from the high-temperature ($T > T_K$) behaviour of $\rho(T)$ and $\chi(T)$ [1, 11, 22] and decreases rapidly with increasing x, as noted above. Over relatively wide ranges of x ($\sim$ 0.05–0.2) and T (at least two decades), the U 5f electron contributions to these properties, $\Delta\rho(T)$, $\Delta C(T)$, and $\Delta\chi(T)$, in the limit $T \ll T_K$, can be described by the following expressions:

$$\Delta\rho(T)/\Delta\rho(0) = 1 - a(T/T_K) \tag{3}$$

$$\Delta C(T)/T = (-bR/T_K)\ \ln[b'(T/T_K)] \tag{4}$$

$$\Delta\chi(T)/\Delta\chi(0) = 1 - c(T/T_K)^{1/2}. \tag{5}$$

The constants ay, b, b', and c which appear in (3)–(5) were determined from $\rho(T)$, $C(T)$, and $\chi(T)$ data for a $Y_{1-x}U_xPd_3$ sample with $x = 0.2$, as follows. Equation (4) has the same form as the two-channel spin-$\frac{1}{2}$ Kondo formula in which b and b' have the values 0.25 and 2.4, respectively [20]. Analysis of the $C(T)/T$ data for a sample with $x = 0.2$ using (4) with these values of b and b' yielded $T_K = 42$ K. This value of T_K is close to the value of T_K inferred from the electrical resistivity at higher temperatures according to the criterion $\Delta\rho(T_K)/\Delta\rho(0) \equiv 0.8$ (T_K is the temperature where $\Delta\rho(T)$ starts to deviate from a $\log T$ dependence). The values $a = 0.23$ and $c = 0.36$ in (3) and (5) were determined from the $\Delta\rho(T)$ and $\Delta\chi(T)$ data for the specimen with $x = 0.2$ by setting T_K in (3) and (5) equal to 42 K. However, we would like to emphasize that our use of the two-channel spin-$\frac{1}{2}$ Kondo model values for b and b' in (4) is only phenomenological and not meant to imply that the model can account for all of the NFL characteristics of the $Y_{1-x}U_xPd_3$ system. In summary, the constants $a = 0.23$, $b = 0.25$, $b' = 2.4$, and $c = 0.36$ in (3)–(5) yield values of T_K from the low-temperature behaviour of $\Delta\rho(T)$, $\Delta C(T)$, and $\Delta\chi(T)$ that are consistent with the value of T_K from the high-temperature behaviour of $\Delta\rho(T)$ for $x = 0.2$. These values of a, b, b', and c are used in the following to extract values of T_K from the low-temperature behaviour of $\Delta\rho(T)$, $\Delta C(T)$, and $\Delta\chi(T)$ for *all other values* of x.

Shown in figures 4(a)–(c) are $\Delta\rho(T)$, $\Delta C(T)$, and $\Delta\chi(T)$ data respectively for an $Y_{1-x}U_xPd_3$ specimen with $x = 0.2$. The $\Delta\rho(T)$ data for this specimen can be fitted by the relation

$$\Delta\rho(T)/\Delta\rho(0) = 1 - a(T/T_K)^n \tag{6}$$

where $\Delta\rho(0)$, n, and T_K are adjustable fitting parameters. The best fit yields the value $n = 1.1 \pm 0.1$. The $\Delta C(T)/T$ data are described well by (4) in the range 0.3 K $< T \leqslant 10$ K, but deviate from it below 0.3 K as shown in figure 4(b). Within the context of a two-channel spin-$\frac{1}{2}$ Kondo model, this upturn in $\Delta C(T)/T$ could be due to a lifting of the degeneracy of a U^{4+} doublet groundstate by an exchange field or the CEF due to changes in local symmetry, which could remove the residual $(R/2)\ \ln 2$ entropy. The $\Delta\chi(T)$ data

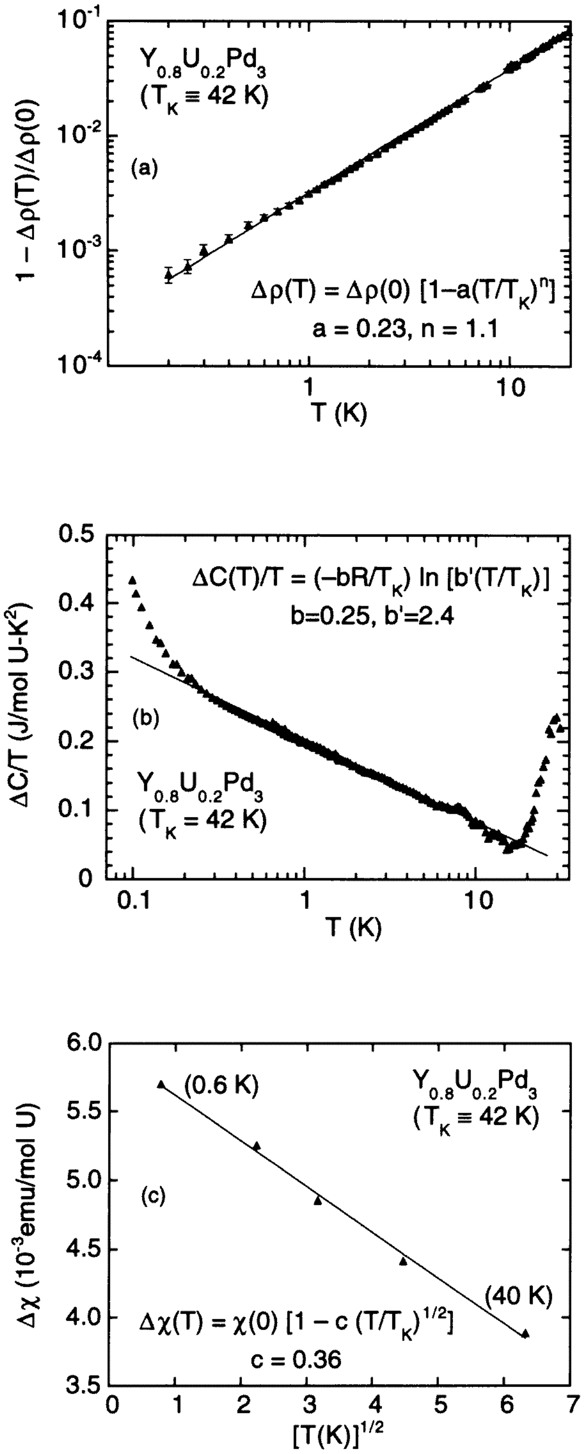

Figure 4. The U contribution to the electrical resistivity, $\Delta\rho$, specific heat, ΔC, and magnetic susceptibility, $\Delta\chi$, of $Y_{0.8}U_{0.2}Pd_3$, plotted as (a) $\log[1 - \Delta\rho(T)/\Delta\rho(0)]$ against $\log T$, $(b)\Delta C(T)/T$ against $\log T$, and (c) $\Delta\chi$ against $T^{1/2}$.

can be fitted between 0.6 and 40 K by (5), after the $M(H, T)$ data have been corrected by removing a nonlinear contribution that scales with $H/(T - \theta)$ and was assumed to be due to magnetic impurities [1].

Previous measurements of $\rho(T)$ for $Y_{1-x}U_xPd_3$ over the range $0.02 \leqslant x \leqslant 0.2$ down to $\sim$1.2 K are consistent with (6) with $n = 1.0 \pm 0.1$. Currently, we are in the process of extending our measurements of $\rho(T)$, $C(T)$, and $\chi(T)$ for the $Y_{1-x}U_xPd_3$ system to lower values of x and T. The purpose of these experiments is to determine the range of x and T over which (3)–(5) provide an adequate description of the data.

Shown in figure 5(a)–(c) are $\Delta\rho(T)$ data for $Y_{1-x}U_xPd_3$ specimens with $x = 0.2$, 0.15, and 0.1, respectively. The $\Delta\rho(T)$ data for $x = 0.2$ are the same as those shown in figure 4(a), while the $\rho(T)$ data for $x = 0.1$ and 0.15 are new measurements down to $\sim$100 mK. The best overall fits of these data to (6) with $a = 0.23$ yield values of $T_K = 142$ K and $n = 1.4$ for $x = 0.10$ and $T_K = 95$ K and $n = 1.1$ for $x = 0.15$. These data indicate that the values of T_K extracted from the low-temperature $\Delta\rho(T)$ data decrease with increasing x and generally track the T_K values determined from the high-temperature $\Delta\rho(T)$ data. This strongly suggests that the NFL behaviour at low temperature is associated with the Kondo effect that is evident in the high-temperature $\Delta\rho(T)$ and $\Delta\chi(T)$ data. The value of n increases from ~ 1 for $x = 0.20$ and 0.15 to ~ 1.4 for $x = 0.1$, although this exponent is very sensitive to the low-temperature measurements, which are subject to greater uncertainty due to the small measuring currents that are required to reduce Joule heating at the contacts between the electrical leads and the samples. Further experiments are needed to determine how the exponent n varies at lower concentration and whether it increases to two, indicating a crossover to a Fermi liquid for low x. According to a recent study of the transport, thermal, and magnetic properties of the $Y_{1-x}U_xPd_3$ system by Aoki *et al* [26], this system behaves as a Fermi liquid below $x \approx 0.1$. The present investigation indicates that the crossover, if it exists at all, is below $x = 0.1$.

Displayed in figures 6(a)–(c) are $\Delta\rho(T)$, $\Delta C(T)$, and $\Delta\chi(T)$ data respectively for a $Y_{1-x}U_xPd_3$ specimen with $x = 0.1$. The $\Delta\rho(T)$ data in figure 6(a) are the same as those shown in figure 5(c). The $\Delta C(T)/T$ data can be described by (4), but deviate from the $\log T$ behaviour below ~ 0.3 K in a manner similar to that for the $\Delta C(T)/T$ data for the $x = 0.2$ sample in figure 4(b). Using the values for b and b' from the two-channel spin-$\frac{1}{2}$ Kondo model, the fit yields a value $T_K = 224$ K, again consistent with the general decrease of T_K with increasing x reflected in the high-temperature $\Delta\rho(T)$ and $\Delta\chi(T)$ data. Similarly, $\Delta\chi(T)$ shown in figure 5(c), after correcting for a small saturable contribution to $M(H, T)$, is consistent with (5), although the $\Delta\chi(T)$ data show some tendency to saturate below ~ 5 K. Using the value $c = 0.36$, determined from the $x = 0.2$ data as described above, the fit yields a value of $T_K = 208$ K, again consistent with the Fermi level tuning picture.

The T–x phase diagram for the $Y_{1-x}U_xPd_3$ system is shown again in figure 7 with a logarithmic temperature scale, with the values of T_K determined from the high-temperature $\Delta\rho(T)$ and $\Delta\chi(T)$ data, which we denote as T_K—ρ_{HT} and $\theta_p/3$ (using the result $\theta_p = -cT_K$, where $c \approx$ 3–4), and the low-temperature values of T_K extracted from the $\Delta\rho(T)$, $\Delta C(T)$, and $\Delta\chi(T)$ data, which we denote as T_K—ρ_{LT}, T_K—C/T, and T_K—χ_{LT}. Given the uncertainties in estimating values of T_K, the T_K–x data in figure 7 are consistent with a scaling of the low-temperature NFL characteristics with the Kondo temperature T_K, inferred from high-temperature properties. The plot of T_K–x in figure 7 is also consistent with a linear decrease of $\ln T_K$ with increasing x, or, an *exponential* decrease of T_K with increasing x, as expected from Fermi level tuning. Thus, on the basis of these experiments, the NFL characteristics in the low-temperature physical properties of the system appear to

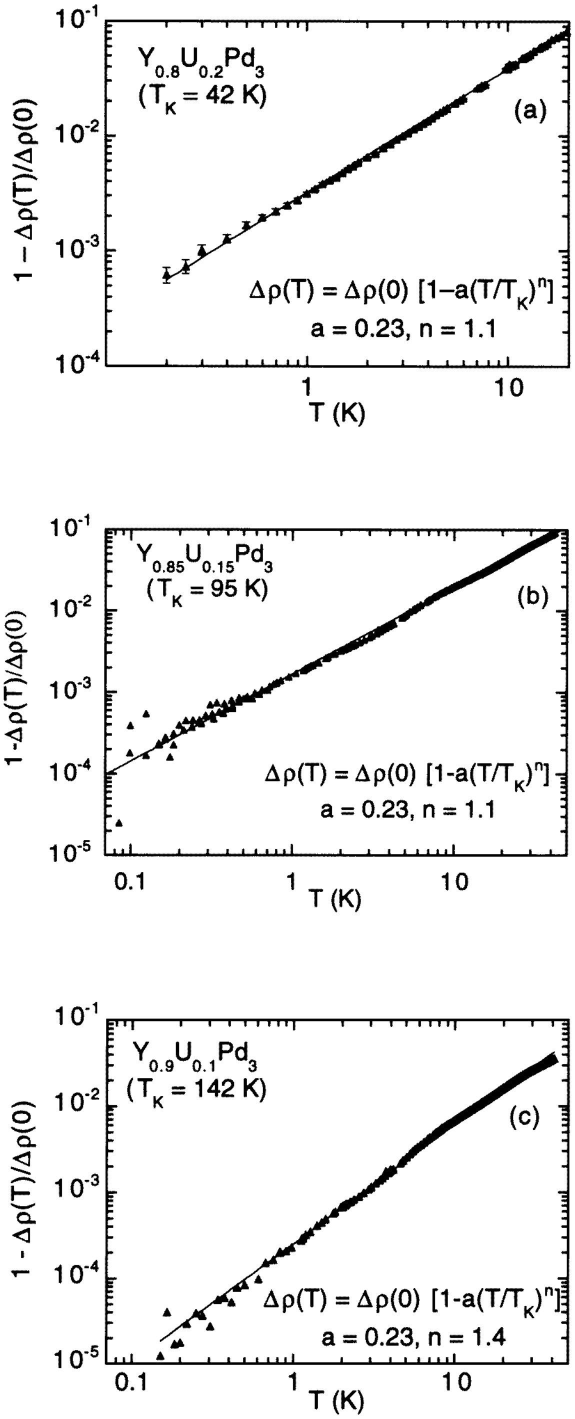

Figure 5. The U contribution to the electrical resistivity, $\Delta\rho$, of $Y_{1-x}U_xPd_3$ ((a) $x = 0.2$; (b) 0.15; and (c) 0.1), plotted as $\log[1 - \Delta\rho(T)/\Delta\rho(0)]$ against $\log T$.

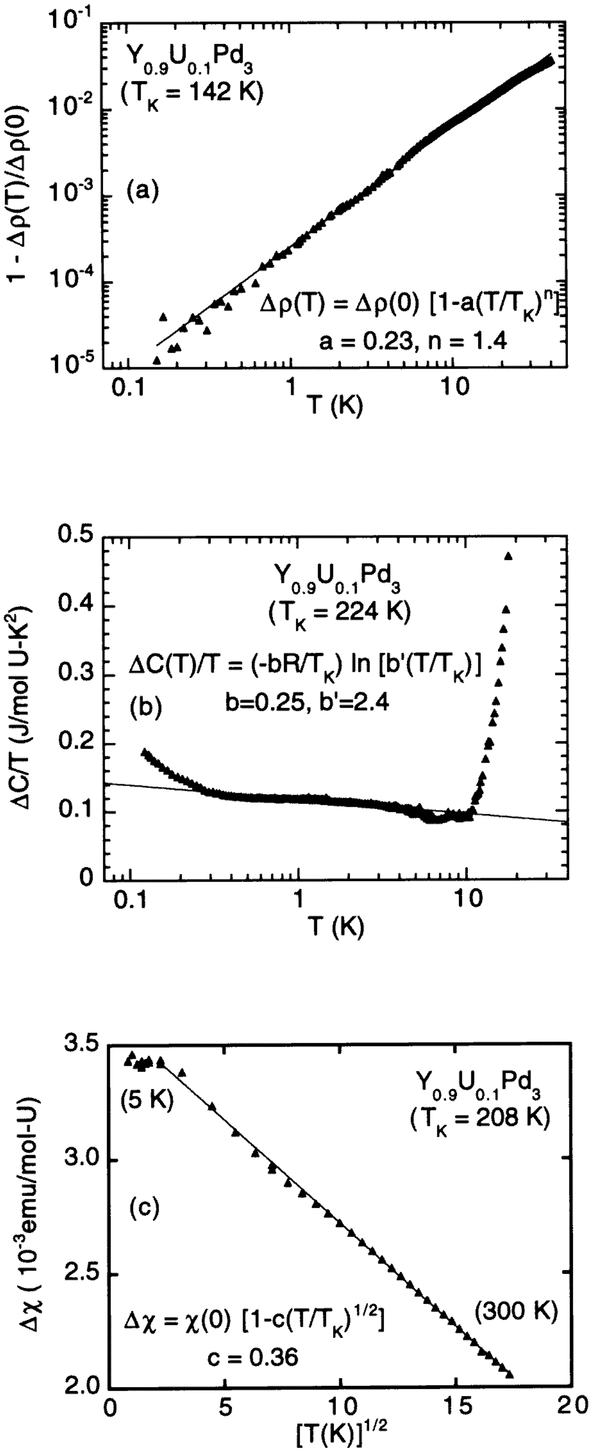

Figure 6. The U contribution to the electrical resistivity, $\Delta\rho$, specific heat, ΔC, and magnetic susceptibility, $\Delta\chi$, of $Y_{0.9}U_{0.1}Pd_3$, plotted as (a) $\log[1 - \Delta\rho(T)/\Delta\rho(0)]$ against $\log T$, (b) $\Delta C(T)/T$ against $\log T$, and (c) $\Delta\chi$ against $T^{1/2}$.

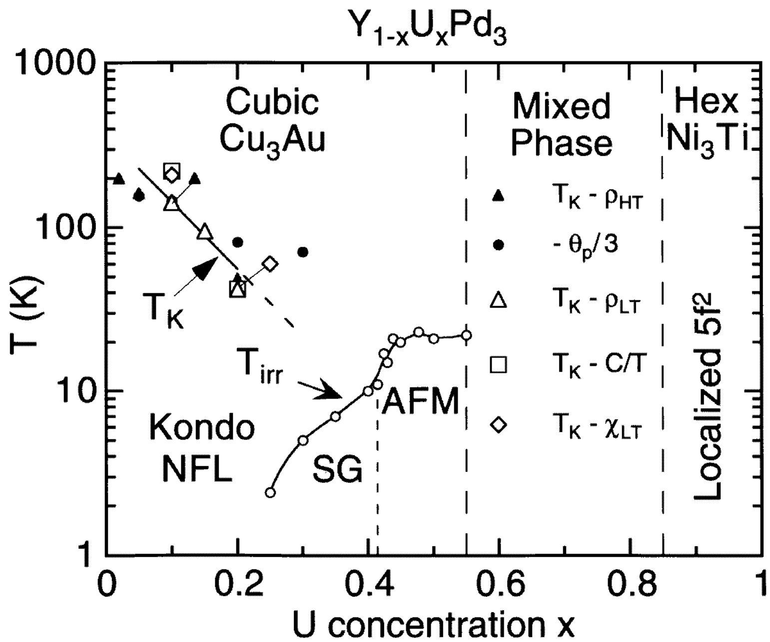

Figure 7. The low-temperature T–x phase diagram for the $Y_{1-x}U_xPd_3$ system, plotted on a logarithmic temperature scale. Kondo temperatures T_K estimated from the high-temperature electrical resistivity and magnetic susceptibility (ρ_{HT}, $-\theta_p/3$) and the low-temperature electrical resistivity, specific heat , and magnetic susceptibility (ρ_{LT}, C/T, χ_{LT}) (see the text) are indicated in the figure.

scale with U concentration x and T_K, suggesting that the origin of the NFL behaviour in this system is a single-ion mechanism, such as a multichannel Kondo effect.

6. The crystalline electric field ground state of U^{4+} in the $Y_{1-x}U_xPd_3$ system

A prerequisite for developing a microscopic model for the NFL behaviour in the low-temperature physical properties of $Y_{1-x}U_xPd_3$ is knowledge of the groundstate and low-lying excited states of U^{4+} in the cubic CEF. The most powerful method of establishing the energy level scheme of localized f states of rare earth or actinide ions in the CEF is inelastic neutron scattering. In a cubic CEF, the ninefold-degenerate $J = 4$ Hund rule multiplet of U^{4+} is split into Γ_4 and Γ_5 triplets, a Γ_1 singlet, and a Γ_3 nonmagnetic doublet that carries an electric quadrupole moment. If Γ_3 were the groundstate, then the NFL characteristics in the physical properties at low temperature could be associated with a quadrupolar Kondo effect [12], the electric analogue of the magnetic two-channel spin-$\frac{1}{2}$ Kondo effect. According to the quadrupolar Kondo model, the electrical resistivity $\Delta\rho(T)$ should vary as $\Delta\rho(T)/\Delta\rho(0) = 1 - a(T/T_K)^{1/2}$ [27], a result that is clearly at variance with the experimentally observed linear T dependence described by (3). On the other hand, the quadrupolar Kondo model predicts that the specific heat $\Delta C(T)$ [25] and the magnetic susceptibility $\Delta\chi(T)$ [28] have the same forms as (4) and (5), respectively, both of which are consistent with experiment [1, 2, 22]. In (5), $\Delta\chi(0)$ is the van Vleck susceptibility between the Γ_3 groundstate and the first excited CEF state. The value of $\Delta\chi(0)$ obtained by fitting

(5) to $\Delta\chi(T)$ for $x = 0.2$ is comparable to the calculated van Vleck susceptibility between the Γ_3 groundstate and the Γ_5 first excited CEF state at 7 meV inferred from inelastic neutron scattering measurements on $Y_{0.8}U_{0.2}Pd_3$ by Mook *et al* [29]. The conclusion that the groundstate is the Γ_3 nonmagnetic doublet was based on the small quasielastic line width $\Delta/2 \lesssim 0.1$ meV which is significantly smaller than the $k_B T_K \sim 4$ meV value expected for a Kondo effect of magnetic origin. When the NFL behaviour of $Y_{1-x}U_xPd_3$ was first reported [11], the $T^{1/2}$ variation of $\Delta\rho$ had not yet been established theoretically and arguments were advanced that $\Delta\rho$ should have a linear T dependence. Thus, it appeared that the NFL behaviour of $Y_{1-x}U_xPd_3$ could be explained in terms of a quadrupolar Kondo effect.

Recently, Dai *et al* [18] performed polarized inelastic neutron scattering (INS) as well as elastic neutron scattering measurements on samples with $x = 0.2$ and 0.45. The polarized INS measurements indicated that the groundstate of U^{4+} in $Y_{0.55}U_{0.45}Pd_3$, and, possibly, also $Y_{0.8}U_{0.2}Pd_3$, is the Γ_5 triplet with an excited state Γ_3 nonmagnetic doublet at 5 meV and a Γ_4 triplet at 39 meV. The quasielastic line width $\Delta/2$ was estimated to be less than 1 meV, still smaller than the value $k_B T_K \sim 4$ meV expected for a magnetic Kondo effect. A magnetic Γ_5 triplet groundstate would exclude the possibility of a quadrupolar Kondo effect, unless the Γ_5 is split at low temperatures due, for example, to a local change in crystal symmetry from cubic to tetragonal or hexagonal [30], or there is a crossover from a Γ_5 groundstate at $x = 0.45$ to a Γ_3 groundstate at $x = 0.2$. It is interesting to note that a crossover or transition in electronic structure near $x = 0.2$ has been inferred by McCarten *et al* [31] from thermoelectric power measurements on $Y_{1-x}U_xPd_3$. Elastic scattering measurements on the sample with $x = 0.45$ revealed the occurrence of long-range AFM order with a Néel temperature $T_N = 21$ K and an ordered moment $\mu = 0.7\,\mu_B$/U. The AFM structure is the same as that of the compound UPd_4, which also has the cubic Cu_3Au crystal structure, and involves a doubling of the chemical unit cell in two directions. The magnetization $M(T)$ was found to be reversible and to vary as $[M(T)/M(0)]^2 = (1 - T/T_N)^{0.7}$. Neutron scattering measurements on the sample with $x = 0.2$ did not indicate any magnetic order above 0.2 K. However, critical fluctuations associated with AFM ordering with the same wave vector as the $x = 0.45$ sample were observed on cooling from 77 to 0.2 K.

A metallurgical study of selected $Y_{1-x}U_xPd_3$ samples in the range $0 \leqslant x \leqslant 0.2$ by means of electron probe microanalysis by Süllow *et al* [32] revealed local variations of the composition parameter x of up to 30% of the nominal concentration on a scale of $10\,\mu$m for arc-melted and unannealed samples, such as those used in the present investigation. We have also observed U concentration fluctuations, although they appear to be smaller than those reported in [32], and changes in microstructure as x is varied in the $Y_{1-x}U_xPd_3$ system in our ongoing investigation which will be reported on at a later date.

Thus, the situation in the $Y_{1-x}U_xPd_3$ system seems to be considerably more complex than originally envisaged, and no single model appears to be able to account for all of its varied and unusual properties. While an unconventional Kondo effect would seem to provide a natural explanation for the scaling of the NFL characteristics with T_K, we cannot rule out the possibility that the NFL behaviour is associated with the spin glass phase that forms in the interval $0.2 \lesssim x \lesssim 0.43$. However, the persistence of the NFL behaviour over a relatively large range of x values $\lesssim 0.2$ would seem to be difficult to accommodate in a spin glass scenario. Although the mechanisms responsible for the NFL behaviour in the $Y_{1-x}U_xPd_3$ system have not yet been definitively established, the extraordinary properties of this system stimulated the search for other f-electron systems that exhibit NFL behaviour at low temperatures and the investigation of their physical properties, as well as the development of various theoretical models.

7. Recent experiments on the $U_{1-x}M_xPd_2Al_3$ (M = Th, Y) system

Another interesting example of NFL behaviour in a strongly correlated f-electron system is found in $U_{1-x}Th_xPd_2Al_3$ in the concentration range $0.4 \lesssim x < 1$ where an unconventional Kondo effect is observed [1]. The parent compound UPd_2Al_3 is a heavy-fermion AFM superconductor with $T_N = 14.6$ K and $T_c \approx 2$ K that crystallizes in the hexagonal $PrNi_2Al_3$ structure [33]. The ordered moment of UPd_2Al_3 is relatively large (0.85 μ_B), and the AFM structure of UPd_2Al_3 consists of alternating ferromagnetic sheets, with the moments lying in the hexagonal basal plane [34]. The temperature dependence of the upper critical field is consistent with singlet superconductivity, and the AFM transition appears to involve the opening of a 30 meV gap over part of the Fermi surface [35], similar to that observed in URu_2Si_2 [36].

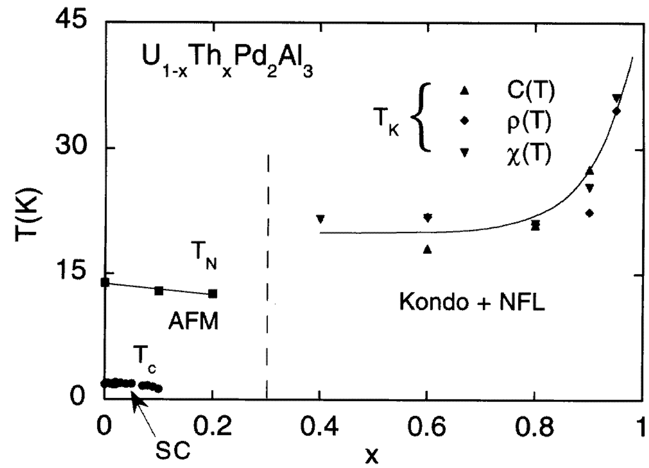

Figure 8. The low temperature T–x phase diagram for the $U_{1-x}Th_xPd_2Al_3$ system. The line on the right-hand side of the figure represents the estimated value of the Kondo temperature T_K inferred from the $\rho(T)$, $C(T)$, and $\chi(T)$ data. (After [1].)

The low-temperature T–x phase diagram of $U_{1-x}Th_xPd_2Al_3$, based upon measurements of $\rho(T)$, $C(T)$, and $\chi(T)$, is shown in figure 8 [1]. As the Th concentration x is increased, T_N and T_c decrease only slightly, but the features associated with AFM and superconductivity are rapidly suppressed and eventually become undetectable. The line on the right-hand side of the figure represents the estimated value of the Kondo temperature T_K, inferred from $\rho(T)$, $C(T)$, and $\chi(T)$.

Electrical resistivity $\rho(T)$ measurements on the $U_{1-x}Th_xPd_2Al_3$ system reveal Kondo-like behaviour in which the contribution due to scattering from the U ions increases with decreasing temperature. However, the Kondo-like behaviour in the range $0.4 \lesssim x \lesssim 1$ appears to be unconventional in the sense that the U contribution to $\rho(T)$ is linear between a few kelvins and about 20 K, similar to that of the $M_{1-x}U_xPd_3$ (M = Sc, Y) system [1, 2, 18]. At temperatures below a few kelvins, $\rho(T)$ levels off, indicating a crossover from NFL to Fermi-liquid (FL) behaviour as the temperature decreases. Within the context of a multichannel Kondo model, this would suggest that the degeneracy of the conduction electron channels or the localized electron spin or charge degrees of freedom has been lifted by some residual interaction, producing an evolution towards single-channel behaviour. In the range 4 K $\leqslant T \leqslant$ 20 K, the U contribution to the resistivity can be described by the relation $\Delta\rho(T)/\Delta\rho(0) = 1 - a(T/T_K)^n$ with $n \approx 1$ and $a = 0.1$ for T_K values consistent with those inferred from the specific heat for various values of x between 0.6 and 0.95. This is illustrated in the $\log[1 - \Delta\rho(T)/\Delta\rho(0)]$ against $\log(T/T_K)$ plot of figure 9(a), where the values of T_K for $a = 0.1$ are listed.

Displayed in figure 10 are plots of C/T (J(mol U)$^{-1}$ K^{-2}) against $\log T$ for the $U_{1-x}Th_xPd_2Al_3$ system with $x = 0.4$, 0.6, and 0.8 down to $\sim$100 mK. Analysis of the specific heat data in terms of the two-channel spin-$\frac{1}{2}$ Kondo formula yields values of T_K of $\sim$20 K. In contrast to the $Y_{1-x}U_xPd_3$ system, there is no deviation of C/T above the $\log T$ behaviour below $\sim$0.3 K.

For values of $x \gtrsim 0.2$, $\chi(T)$ follows a Curie–Weiss law between $\sim$50 and 300 K; the effective magnetic moment μ_{eff} and Curie–Weiss temperature θ_p vary somewhat with x and have values $\mu_{eff} \approx 2.4\mu_B$ and $\theta_p \approx -40$ K in the NFL regime $x \gtrsim 0.4$. Since, for Kondo systems, $|\theta_p| \approx 3 - 4T_K$, this suggests a value $T_K \approx 10$ K, in reasonable agreement with values of T_K obtained from the scaling of the electrical resistivity and specific heat. At the lowest temperatures, the $\chi(T)$ data are consistent with the relation $\chi(T)/\chi(0) = 1 - c(T/T_K)^{1/2}$, with values of T_K for $c = 1.15$ that are in reasonable agreement with those obtained from $\rho(T)$ and $C(T)$. A plot of $\chi(T)/\chi(0)$ against $(T/T_K)^{1/2}$ for several samples in the range $0.6 \leqslant x \leqslant 0.95$ appears in figure 9(b).

Recently, optical investigations of the $U_{1-x}Th_xPd_2Al_3$ ($0 \leqslant x < 0.9$) system were carried out over a broad frequency ω range from 15 to 10^5 cm^{-1} by Degiorgi *et al* [37]. The frequency dependence of the scattering relaxation rate $\Gamma(\omega)$ at low temperatures was observed to evolve from a FL-like ω^2 behaviour for $x \lesssim 0.2$ to a NFL-like ω-linear dependence for $0.4 \lesssim x \lesssim 0.9$.

Shown in figure 11 are normalized U contribution to the resistivity, $\Delta\rho(T)/\Delta\rho$(293 K), against T data we recently obtained for the $U_{1-x}Y_xPd_2Al_3$ system with $x = 0.1$, 0.2, 0.6, and 0.8. The $\Delta\rho(T)/\Delta\rho$ (293 K) against T curves for the samples with $x = 0.6$ and 0.8 in the NFL regime exhibit pronounced maxima and then decrease linearly with T, as shown in the inset of figure 11. This behaviour is in sharp contrast to that observed for the $U_{1-x}Th_xPd_2Al_3$ system and appears to be another case where the resistivity is linear in T at low temperature, but with $a < 0$. Further research on the $U_{1-x}Y_xPd_2Al_3$ system is currently in progress, and will yield an interesting comparison to the Th-substituted UPd_2Al_3 system.

8. Concluding remarks

The $Y_{1-x}U_xPd_3$ system exhibits a rich variety of phenomena in the cubic Cu_3Au phase ($0 < x \lesssim 0.55$) which includes an unconventional Kondo effect, Fermi level tuning of the Kondo temperature, CEF effects, NFL behaviour of the physical properties at low temperatures for $0 < x \lesssim 0.2$, and spin glass and long-range AFM order in the range $0.2 \lesssim x \lesssim 0.55$. The electrical resistivity $\Delta\rho(T)$, specific heat $\Delta C(T)$, and magnetic susceptibility $\Delta\chi(T)$ scale with T_K, suggesting that they are associated with an unconventional Kondo effect. However, neither a magnetic nor an electric (quadrupolar) two-channel spin-$\frac{1}{2}$ Kondo effect can account for all of the observed NFL characteristics, at least at the present level of understanding of these models. Chemical disorder may also play an important role. An interesting example in which NFL behaviour is induced by substituting a nonmagnetic element (Th or Y) into a heavy-fermion AFM superconductor (UPd_2Al_3) is provided by the $U_{1-x}M_xPd_2Al_3$ (M = Th, Y) system. In this system, $\Delta\rho(T)$, $\Delta C(T)$, and $\Delta\chi(T)$ also scale with T_K, suggesting that they are associated with an unconventional Kondo effect. It is interesting to note that single-ion scaling of the specific heat and

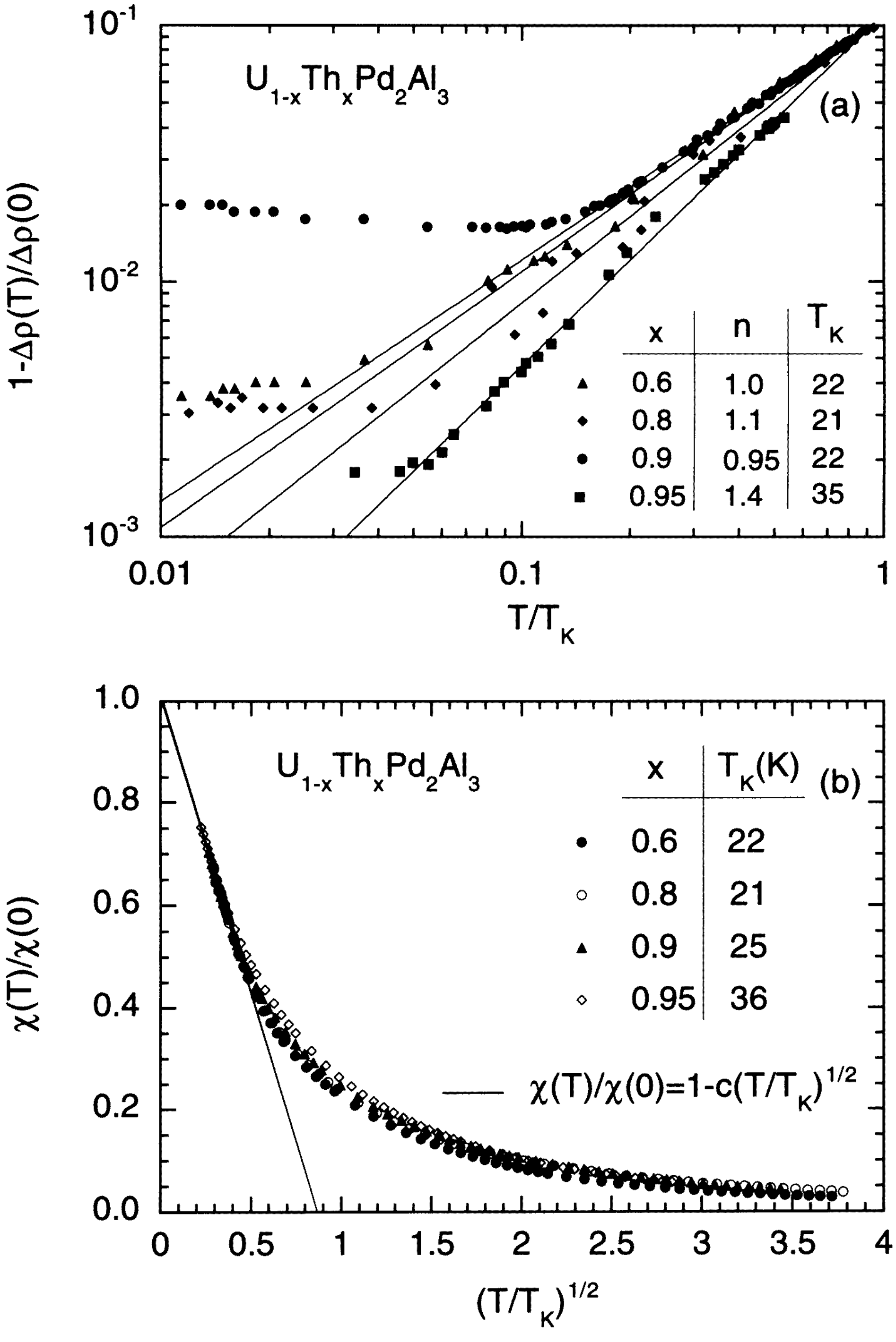

Figure 9. The U contribution to (a) the electrical resistivity, $\Delta\rho(T)$, plotted as $\log[1 - \Delta\rho(T)/\Delta\rho(0)]$ against $\log T$, and (b) the magnetic susceptibility, $\Delta\chi(T)$, plotted as $\Delta\chi(T)/\Delta\chi(0)$ against $(T/T_K)^{1/2}$, for various $U_{1-x}Th_xPd_2Al_3$ alloys.

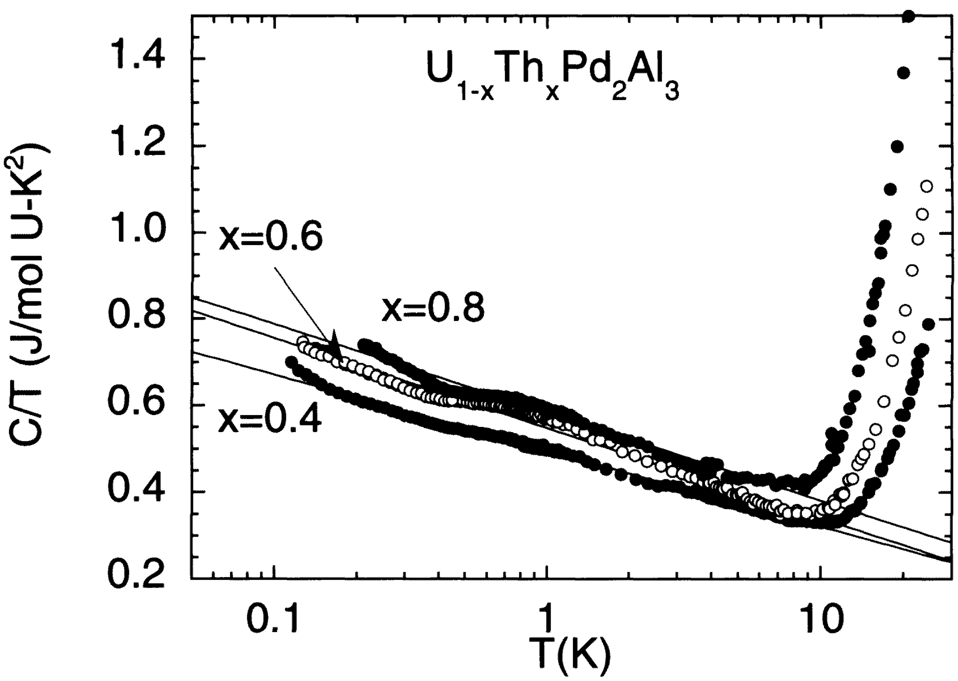

Figure 10. The low-temperature specific heat per mole U divided by temperature, C/T, against $\log T$ for $U_{1-x}Th_xPd_2Al_3$ alloys with $x = 0.4$, 0.6, and 0.8 to temperatures as low as ~ 100 mK. (After [24].)

magnetic susceptibility, both of which exhibit $-\ln T$ behaviour, has been observed in dilute $Th_{1-x}U_xRu_2Si_2$ ($x \leqslant 0.07$) [38] and $Th_{1-x}U_xPd_2Si_2$ ($x \leqslant 0.07$) [39] alloys. In both of these systems, $\rho(T)$ decreases with decreasing temperature below ~ 4 K, although in the $Th_{1-x}U_xPd_2Si_2$ system the decrease in $\rho(T)$ occurs below a maximum at ~ 5 K, above which $\rho(T)$ increases with decreasing temperature, as it would for a conventional Kondo effect.

The NFL behaviour seems to be a general phenomenon, and more than ten f-electron systems have been found in which $\Delta\rho(T)$, $\Delta C(T)$, and $\Delta\chi(T)$ have temperature dependences given by (3)–(5) that scale with a characteristic temperature T_0, although in some cases the parameter a that appears in the electrical resistivity is negative. As we observed several years ago, these systematics of NFL behaviour appear to be general characteristics of a new class of strongly correlated f-electron materials. In several of these systems, such as the $Y_{1-x}U_xPd_3$ and $U_{1-x}Th_xPd_2Al_3$ systems considered here, the NFL characteristics scale with x and T_K (i.e. $T_K \equiv T_0$), suggesting that the NFL behaviour is associated with an unconventional Kondo effect. On the other hand, in some of these systems, such as $CeCu_{6-x}Au_x$ [4], the NFL behaviour is sharply tuned to the suppression of an AFM transition by varying x or applying pressure, implicating fluctuations of an order parameter above a second-order phase transition at 0 K as the underlying mechanism for the NFL behaviour. Along with the Kondo disorder approach that has recently been proposed to account for certain NFL characteristics in the $UCu_{5-x}Pd_x$ system [40, 41], there appear to be a number of possible routes to NFL behaviour in f-electron systems. However, none of the

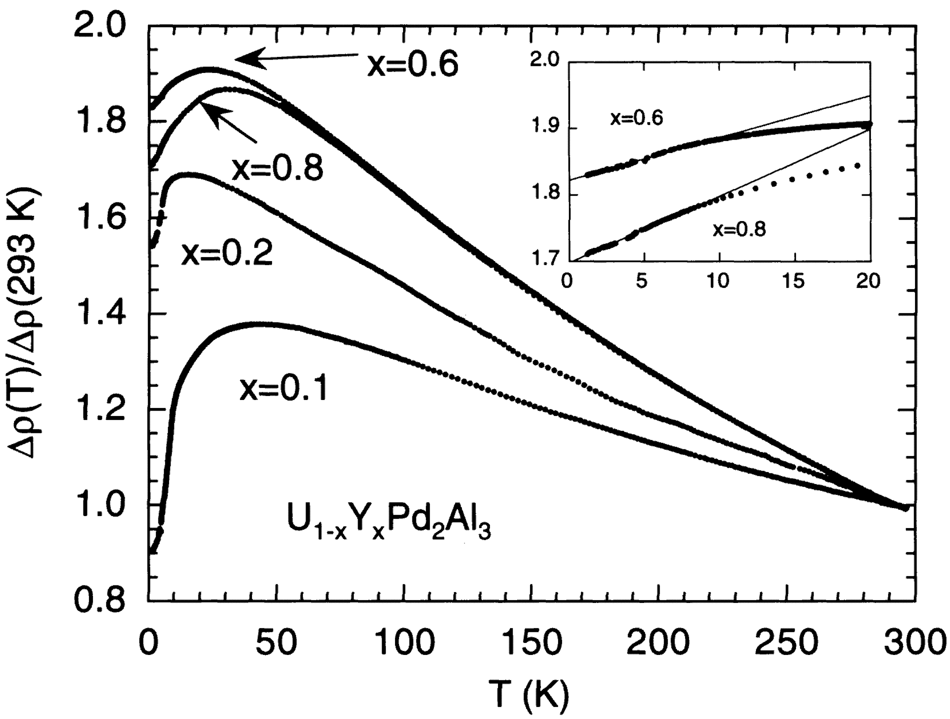

Figure 11. The normalized U contribution to the electrical resistivity $\Delta\rho(T)/\Delta\rho(293\text{ K})$ of $U_{1-x}Y_xPd_2Al_3$ alloys with $x = 0.1$, 0.2, 0.6, and 0.8. The low-temperature data for the samples with $x = 0.6$ and 0.8 are shown in the inset.

current models seems to be capable of providing a definitive description of all of the NFL characteristics in a single f-electron system. Clearly, much experimental and theoretical work will be required to resolve the various issues associated with this fascinating problem.

Acknowledgments

Research at UCSD was supported by the US National Science Foundation under grant No DMR-94-08835 and the US Department of Energy under grant No DE-FG03-86ER45230. The research at UCSB was partially supported by the National Science Foundation under grant No PHY-94-07194.

References

[1] Maple M B, Seaman C L, Gajewski D A, Dalichaouch Y, Barbetta V B, de Andrade M C, Mook H A, Lukefahr H G, Bernal O O and McLaughlin D E 1994 *J. Low Temp. Phys.* **95** 225
[2] Maple M B, de Andrade M C, Herrmann J, Dalichaouch Y, Gajewski D A, Seaman C L, Chau R, Movshovich R, Aronson M C and Osborn R 1995 *J. Low Temp. Phys.* **99** 223
[3] Andraka B 1994 *Physica* B **199 & 200** 239
[4] von Löhneysen H 1995 *Physica* B **206 & 207** 101
[5] Cox D L 1987 *Phys. Rev. Lett.* **59** 1240
[6] Steglich F, Buschinger B, Gegenwart P, Lohmann M, Helfrich R, Langhammer C, Hellmann P, Donnevert L, Thomas S, Link A, Geibel C, Lang M, Sparn G and Assmus W 1996 *J. Phys.: Condens. Matter* **8** 9909–21

[7] Umeo K, Kadomatsu H and Takabatake T 1996 *J. Phys.: Condens. Matter* **8** 9743–57
[8] Nozieres P and Blandin A 1980 *J. Physique* **41** 193
[9] See, e.g. Millis A J 1993 *Phys. Rev.* B **48** 7183
Continentino M A 1993 *Phys. Rev.* B **47** 11 587
Tsvelik A M and Reizer M 1993 *Phys. Rev.* B **48** 9887
[10] Cox D L and Maple M B 1995 *Phys. Today* **February** 32
[11] Seaman C L, Maple M B, Lee B W, Ghamaty S, Torikachvili M, S Kang J-S, Liu L Z, Allen J W and Cox D L 1991 *Phys. Rev. Lett.* **67** 2882; 1992 *J. Alloys Compounds* **181** 327
[12] Cox D L 1987 *Phys. Rev. Lett.* **59** 1240
[13] Andraka B and Tsvelik A M 1991 *Phys. Rev. Lett.* **67** 2886
[14] See e.g. Buyers W J L and Holden T M 1985 *Handbook on the Physics and Chemistry of the Actinides* ed A J Freeman and G H Lander (Amsterdam: Elsevier) p 239
[15] Andres K, Davidov D, Dernier P, Hsu F, Reed W A and Niewenhuys G J 1978 *Solid State Commun.* **28** 405
[16] Baer Y, Ott H R and Andres K 1980 *Solid State Commun.* **36** 387
Reihl B, Martensson N, Eastman D E, Arko A J and Vogt O 1982 *Phys. Rev.* B **26** 1842
[17] McEwen K A, Steigenberger U and Martinez J L 1992 *Physica* B **186–188** 670
[18] Dai P, Mook H A, Seaman C L, Maple M B and Koster J P 1995 *Phys. Rev. Lett.* **75** 1202
[19] Wu W D, Keren A, Le L P, Luke G M, Sternlieb B J, Uemura Y, J Seaman C L, Dalichaouch Y and Maple M B 1994 *Phys. Rev. Lett.* **72** 3722
[20] Gajewski D A, Dilley N R, Chau R and Maple M B 1996 *J. Phys.: Condens. Matter* **8** 9793–806
[21] Lòpez de la Torre M A, Rodriguez Fernandez J and McEwen K A 1986 *J. Appl. Phys.* **79** 6364
[22] Seaman C L and Maple M B 1994 *Physica* B **199 & 200** 396
[23] Kang J-S, Allen J W, Maple M B, Torikachvili M S, Ellis W P, Pate B B, Shen Z-X, Yeh J J and Lindau I 1989 *Phys. Rev.* B **39** 13529
[24] Maple M B, Gajewski D A, Chau R, Dai P, Mook H A, Movshovich R and Seaman C L 1996 *Physica* B 223 & 224 447
[25] Tsvelik A M 1985 *J. Phys. C: Solid State Phys.* **18** 159
Sacramento P D and Schlottmann P 1989 *Phys. Lett.* **142A** 245
[26] Aoki Y, Terayama K, Sato H, Maeda K and Onuki Y 1995 *Physica* B **206 & 207** 451
[27] Ludwig A W W and Affleck I 1991 *Phys. Rev. Lett.* **67** 3160
[28] Cox D L and Makivic M 1994 *Physica* B **199 & 200** 391
[29] Mook H A, Seaman C L, Maple M B, Lòpez de la Torre M A, Cox D L and Makivic M 1993 *Physica* B **186–188** 341
[30] Cox D L 1993 *Physica* B **186–188** 312
[31] McCarten J, Brown S E, Seaman C L and Maple M B 1994 *Phys. Rev.* B **49** 6400
[32] Süllow S, Gortenmulder T J, Niewenhuys G J, Menovsky A A and Mydosh J A 1994 *J. Alloys Compounds* **215** 223
[33] Geibel C, Schank C, Thies S, Kitazawa H, Bredl C D, Böhm A, Rau M, Grauel A, Caspary R, Helfrich R, Ahlheim U, Weber G and Steglich F 1991 *Z. Phys.* B **84** 1
[34] Krimmel A, Fischer P, Roessli B, Maletta H, Geibel C, Schank C, Graul A, Loidl A and Steglich F 1991 *Z. Phys.* B **86** 161
[35] Dalichaouch Y, de Andrade M C and Maple M B1992 *Phys. Rev.* B **43** 299
[36] Maple M B, Chen J W, Dalichaouch Y, Kohara T, Rossel C, Torikachvili M S, McElfresh M W and Thompson J D 1986 *Phys. Rev. Lett.* **56** 185
[37] Degiorgi L, Wachter P, Maple M B, de Andrade M C and Herrmann J 1996 *Phys. Rev.* B at press
[38] Amitsuka H, Hidano T, Honma T, Mitamura H and Sakakibara T 1993 *Physica* B **186–188** 337
[39] Amitsuka H, Shimamoto T, Honma T and Sakakibara T 1995 *Physica* B **206 & 207** 461
[40] Bernal O O, MacLaughlin D E, Lukefahr H G and Andraka A 1995 *Phys. Rev. Lett.* **75** 2023
[41] Miranda E, Dobrosavljevic V and Kotliar G *J. Phys.: Condens. Matter J. Phys.: Condens. Matter* **8** 9871–900